

Wilson Renormalization Group Study of Inverse Symmetry Breaking

Thomas G. Roos¹

*Newman Laboratory of Nuclear Studies,
Cornell University, Ithaca, NY 14853*

Abstract

For a large class of field theories there exist portions of parameter space for which the loop expansion predicts increased symmetry breaking at high temperature. Even though this behavior would clearly have far reaching implications for cosmology such theories have not been fully investigated in the literature. This is at least partially due to the counter intuitive nature of the result, which has led to speculations that it is merely an artifact of perturbation theory. To address this issue we study the simplest model displaying high temperature symmetry breaking using a Wilson renormalization group approach. We find that although the critical temperature is not reliably estimated by the loop expansion the total volume of parameter space which leads to the inverse phase structure is not significantly different from the perturbative prediction. We also investigate the temperature dependence of the coupling constants and find that they run approximately according to their one-loop β -functions at high temperature. Thus, in particular, the quartic coupling of φ^4 theory is shown to increase with temperature, in contrast to the behavior obtained in some previous studies.

¹Electronic address: roost@hepth.cornell.edu

1 Introduction

Intuitively, one expects symmetries that are spontaneously broken at $T = 0$ to be restored at high temperature. Examples of this behavior in condensed matter systems abound, and it was suggested many years ago [1] that the same thing might happen in relativistic field theories. This idea was quickly backed up by calculations [2, 3], which essentially showed that for a general gauge theory with scalars and fermions the quadratic part of the effective potential goes like some combination of coupling constants times T^2 . For theories with simple scalar sectors this combination of couplings is quite generally positive-definite, in which case the minimum of the effective potential lies at the origin of field space for sufficiently high temperatures. At the same time it was also pointed out [2], however, that for certain models the coefficient of the T^2 term may be negative. In this case symmetries are not restored at high temperature, and in fact theories which are symmetric at $T = 0$ may be broken for large T . While such theories are not totally generic, they are by no means contrived: all that is necessary is a sufficiently complicated scalar sector (two multiplets will often suffice) and some constraints on the relative sizes of the couplings in the theory. The latter are usually weak enough so that the allowed values for the couplings occupy a sizable portion of parameter space. To be more precise: a necessary condition for high temperature symmetry breaking is the existence of negative scalar couplings in the Lagrangian. Such couplings, however, are automatically allowed in any model with at least two scalar multiplets, and consequently in almost all extensions of the standard model. The effect of these couplings on the phase structure of a theory depends on the details of the model and must be studied on a case by case basis.

It was quickly realized that theories with symmetry non-restoration or multiple high temperature phase transitions have many attractive phenomenological features. A partial list of applications includes the strong CP problem and GUT scale baryogenesis [4], the monopole problem [5, 6], baryogenesis and dark matter [7], and inflation [8].

In this paper we will not discuss any particular physical application of models that exhibit an inverse phase structure. Instead, we will focus on the phenomenon itself, specifically on the validity of the one-loop calculation that predicts it in the first place. There are several reasons for doing this, perhaps the most important being that there seems to be a widespread suspicion that

symmetry non-restoration is merely an artifact of perturbation theory and not a true physical effect. While this is partially due to the counter intuitive nature of the phenomenon, there is some quantitative evidence to back up this claim. For example, a popular theory whose effective potential predicts an inverse phase structure in the one-loop approximation is the $O(N) \times O(N)$ model [2]. However, subsequent calculations based on large N expansions and Gaussian effective potential techniques seemed to show that the symmetry is in fact restored at high temperature [9]. While the validity of these results is not clear to us, the fact that they incorporate some non-perturbative physics clearly raises the specter that the conclusions drawn from the loop expansion are erroneous.

There are additional reasons to be concerned about the validity of the perturbative calculation of the effective potential. For example, consider the case where the theory is symmetric at $T = 0$, in which case perturbation theory predicts that the symmetry will be broken at high temperature. It is well known that the loop-expansion breaks down in the vicinity of the phase transition due to severe infrared divergences. Now we expect these infrared effects to strongly renormalize the coupling constants in the theory, which is important because the existence of the symmetry breaking transition depends on a certain relationship between these couplings. It is clearly not inconceivable that the renormalization will destroy this relationship and circumvent the transition all together. Even in the case where one starts in the broken phase the situation is not entirely clear-cut. For while the loop-expansion predicts that this symmetry will remain broken at arbitrarily high temperature, it fails to include the effect of the temperature on the coupling constants. Again it is possible that the effective coupling constants appropriate at high temperature do not obey the inequalities required to keep the symmetry broken.

In light of all this it would be nice to study theories which naively admit an inverse phase structure using techniques that: one, capture enough non-perturbative physics to correctly handle the infrared problems in the vicinity of second order (or weakly first order) phase transitions; and two, unambiguously take into account the effects of temperature on the parameters in the theory. Fortunately such a technique has become available in recent years. It is based on an exact renormalization group (RG) equation for the Wilsonian effective action, which has the nice feature that it admits relatively simple approximations that nonetheless capture a good deal of the non-perturbative

physics². Using this tool we will study a $\mathbb{Z}_2 \times \mathbb{Z}_2$ symmetric scalar field theory, the simplest model that exhibits an inverse phase structure in the one-loop approximation. As explained above, our goal will be to test the validity of the perturbative calculation and to establish if high temperature symmetry breaking is in fact possible.

The paper is organized as follows. In section 2 we present a brief derivation of the exact RG equation for the effective action and discuss the approximate version that we will solve. To illustrate the techniques involved, section 3 treats the high temperature phase transition of simple φ^4 theory. In section 4 we then focus on inverse symmetry breaking in the $\mathbb{Z}_2 \times \mathbb{Z}_2$ model. Section 5 discusses the high temperature behavior of coupling constants and its relation to phase transitions. Our results are summarized in section 6.

2 Flow Equation

For completeness we present a brief derivation of the exact renormalization group equation. For details the reader is referred to the literature [10, 11, 12]. We work in D Euclidean dimensions and for simplicity consider a single real scalar field φ . For a theory with action $S[\varphi]$ a scale dependent partition function is defined as (dots represent contractions in function space)

$$\exp W_\Lambda[J] = N \int \mathcal{D}\varphi \exp \left\{ -\frac{1}{2} \varphi \cdot \Delta_\Lambda^{-1} \cdot \varphi - S_{\Lambda_0}[\varphi] + J \cdot \varphi \right\}, \quad (1)$$

where Λ_0 is an ultraviolet cutoff, N is a J independent normalization factor, and

$$\Delta_\Lambda \equiv \frac{\theta_\epsilon(q, \Lambda)}{\theta_\epsilon(\Lambda, q)} \frac{1}{q^2} \quad (2)$$

is a free massless propagator times the ratio of two smooth (everywhere positive) cutoff functions θ_ϵ . This function has the properties

$$\theta_\epsilon(q, \Lambda) \approx 1 \quad \text{for } q > \Lambda + \epsilon$$

and

$$\theta_\epsilon(q, \Lambda) \approx 0 \quad \text{for } q < \Lambda - \epsilon.$$

²See section 2 for details and references.

For later use we note that the sharp cutoff limit is given by the Heaviside function:

$$\lim_{\epsilon \rightarrow 0} \theta_\epsilon(q, \Lambda) = \theta(q - \Lambda) . \quad (3)$$

The effect of the extra term in the exponential of (1) is to suppress the propagation of long wavelength modes ($q^2 \ll \Lambda^2$) while leaving the ultraviolet modes unaffected. In fact it is obvious from (1) that

$$\lim_{\Lambda \rightarrow 0} W_\Lambda[J] = W[J] , \quad (4)$$

the usual generating functional of connected Green's functions. The flow equation for W_Λ is obtained by differentiating (1):

$$\begin{aligned} \frac{\partial W_\Lambda[J]}{\partial \Lambda} = -\frac{1}{2} \left\{ \frac{\delta W_\Lambda}{\delta J} \cdot \frac{\partial \Delta_\Lambda^{-1}}{\partial \Lambda} \cdot \frac{\delta W_\Lambda}{\delta J} \right. \\ \left. + \text{tr} \left(\frac{\partial \Delta_\Lambda^{-1}}{\partial \Lambda} \frac{\delta^2 W_\Lambda}{\delta J \delta J} \right) \right\} . \end{aligned} \quad (5)$$

Now define a scale dependent Legendre effective action via

$$\Gamma_\Lambda[\phi] = -\frac{1}{2} \phi \cdot \Delta_\Lambda^{-1} \cdot \phi - W_\Lambda[J] + J \cdot \phi , \quad (6)$$

where

$$\phi = \frac{\delta W_\Lambda}{\delta J} .$$

In terms of Γ_Λ , (5) becomes

$$\frac{\partial \Gamma_\Lambda[\phi]}{\partial \Lambda} = -\frac{1}{2} \text{tr} \left[\frac{1}{\Delta_\Lambda} \frac{\partial \Delta_\Lambda}{\partial \Lambda} \left(1 + \Delta_\Lambda \frac{\delta^2 \Gamma_\Lambda}{\delta \phi \delta \phi} \right)^{-1} \right] . \quad (7)$$

It is clear from (4) and (6) that

$$\lim_{\Lambda \rightarrow 0} \Gamma_\Lambda[\phi] = \Gamma[\phi] , \quad (8)$$

the generating functional of one particle irreducible (1PI) diagrams. In the opposite limit, $\Lambda \rightarrow \infty$, Δ_Λ^{-1} diverges, so that in (1) the “classical” approximation to $W_\Lambda[J]$ becomes exact. Thus

$$W_\Lambda[J] \rightarrow -S[\phi^*] - \frac{1}{2} \phi^* \cdot \Delta_\Lambda^{-1} \cdot \phi^* + J \cdot \phi^* , \quad (9)$$

where

$$J = \left. \frac{\delta (S[\varphi] + \frac{1}{2}\varphi \cdot \Delta_\Lambda^{-1} \cdot \varphi)}{\delta \varphi} \right|_{\phi^*} .$$

This says simply that as $\Lambda \rightarrow \infty$, W_Λ becomes the Legendre transform of $S + \frac{1}{2}\varphi \cdot \Delta_\Lambda^{-1} \cdot \varphi$. But from (6) $\Gamma_\Lambda + \frac{1}{2}\varphi \cdot \Delta_\Lambda^{-1} \cdot \varphi$ is the Legendre transform of W_Λ , and since $S + \frac{1}{2}\varphi \cdot \Delta_\Lambda^{-1} \cdot \varphi$ is always convex in the limit $\Lambda \rightarrow \infty$, we obtain

$$\lim_{\Lambda \rightarrow \infty} \Gamma_\Lambda[\varphi] = S[\varphi] . \quad (10)$$

We also have the approximate relation

$$\Gamma_{\Lambda_0}[\varphi] = S_{\Lambda_0}[\varphi] , \quad (11)$$

which follows from (10) provided the UV cutoff Λ_0 is sufficiently large compared to all mass scales in S_{Λ_0} . From (8) and (10) we see that Γ_Λ interpolates between the classical action at Λ_0 and the effective action at $\Lambda = 0$. In fact, Γ_Λ has an interpretation as a Wilsonian quantum effective action obtained by integrating out purely quantum modes with momenta $q > \Lambda$ [10].

Equation (7) is exact, but much too complicated to be solved exactly. Its usefulness therefore hinges on the existence of sensible approximation schemes. We begin by writing

$$\begin{aligned} \Gamma_\Lambda = \int d^D x [& U_\Lambda(\varphi) + \frac{1}{2} Z_\Lambda(\varphi) (\partial^\mu \varphi)^2 \\ & + Y_\Lambda(\varphi, (\partial^\mu \varphi)^2) (\partial^\mu \varphi)^4] . \end{aligned} \quad (12)$$

Plugging this into (7), setting φ equal to a constant, and neglecting the φ dependence of Z_Λ we arrive at an approximate evolution equation for the effective potential:

$$\begin{aligned} \frac{\partial U_\Lambda(\varphi)}{\partial \Lambda} = & -\frac{1}{2} \int \frac{d^D q}{(2\pi)^D} \frac{\partial \theta_\epsilon(q, \Lambda)}{\partial \Lambda} \\ & \times \left\{ \theta_\epsilon(q, \Lambda) + \theta_\epsilon^2(q, \Lambda) [Z_\Lambda - 1 + U''_\Lambda(\varphi)/q^2] \right\}^{-1} \end{aligned} \quad (13)$$

(primes denote differentiation with respect to φ). Taking the sharp cutoff

limit (3) and dropping an infinite field independent term we finally obtain³

$$\frac{\partial U_\Lambda(\varphi)}{\partial \Lambda} = -\frac{K_D}{2}\Lambda^{D-1} \ln \left[Z_\Lambda + \frac{U_\Lambda''(\varphi)}{\Lambda^2} \right] , \quad (14)$$

where $K_D = S_{D-1}/(2\pi)^D$, and S_D is the surface area of a unit D-sphere.

This is the equation we will study in the present paper, but before proceeding a few remarks are in order. First note that (13) and (14) have been obtained from the exact result (7) by a truncation of the operator basis. While this is an uncontrolled approximation, the resulting equations have been successfully applied to the study of phase transitions in two, three, and four dimensions, at zero and finite temperature, including the determination of accurate critical exponents [13, 14, 15, 16, 17]. They thus capture a large amount of the relevant physics. It is also possible to show that (14) is simply the first term in a systematic expansion of the exact result[18], which provides some theoretical justification for its remarkable success. Finally, it is interesting to note that if one fixes $U_\Lambda = U_{\Lambda_0}$ and $Z_\Lambda = 1$ on the RHS of (14), and then integrates, the result is simply the well known one-loop effective potential. We emphasize, however, that there are no loop corrections to (14): the use of U_Λ on the RHS corresponds to a resummation of an infinite subset of diagrams, to all orders in the loop expansion.

In this paper we will study the phase structure of four dimensional field theories at finite temperature. We will work with the sharp cutoff equation (14), which, for the purpose at hand, has at least two advantages over its smooth cutoff counterpart: the flow equations are simpler, and there is no dependence on the particular choice of cutoff function. Using the sharp cutoff will also allow us to compare the two approaches since finite temperature phase transitions have been studied using a smooth cutoff in [15, 16].

Specializing now to $D = 4$ and setting $Z_\Lambda = 1$ ⁴, we are faced with the

³Taking the sharp cutoff limit requires some care. We use the relation[10]

$$\frac{\partial \theta_\epsilon(q, \Lambda)}{\partial \Lambda} f(\theta_\epsilon(q, \Lambda), \Lambda) \rightarrow -\delta(\Lambda - q) \int_0^1 dt f(t, q) \quad \text{as } \epsilon \rightarrow 0$$

(here $f(\theta_\epsilon, \Lambda)$ must be continuous at $\Lambda = q$ in dependence on its second argument).

⁴A reasonable approximation for the theories at hand, since the anomalous dimensions are known to be small [14, 17].

task of including finite temperature effects. We begin by writing (14) as

$$\frac{\partial U_\Lambda(\varphi)}{\partial \Lambda} = -\frac{1}{2} \int \frac{d^4 q}{(2\pi)^4} \delta(\Lambda - q) \ln[q^2 + U_\Lambda''(\varphi)] . \quad (15)$$

The imaginary time formalism instructs us to replace

$$\int \frac{d^4 q}{(2\pi)^4} \rightarrow T \sum_{n=-\infty}^{\infty} \int \frac{d^3 q}{(2\pi)^3}$$

and

$$q^2 = q_4^2 + \mathbf{q}^2 \rightarrow \omega_n^2 + \mathbf{q}^2 ,$$

where $\omega_n = 2\pi nT$. This yields

$$\frac{\partial U_\Lambda(\varphi, T)}{\partial \Lambda} = -\frac{K_3}{2} 2\pi T^2 \Lambda g\left(\frac{\Lambda}{T}\right) \ln[\Lambda^2 + U_\Lambda''(\varphi, T)], \quad (16)$$

where

$$g\left(\frac{\Lambda}{T}\right) \equiv \left[\sum_{n=0}^{\left[\frac{\Lambda}{2\pi T}\right]} 2\sqrt{\left(\frac{\Lambda}{2\pi T}\right)^2 - n^2} \right] - \frac{\Lambda}{2\pi T} , \quad (17)$$

and $[x]$ is the greatest integer $\leq x$. We note that $g(x)$ is continuous and piecewise differentiable (see Fig. 1).

It is easy to see that

$$g(x) \rightarrow \frac{x^2}{8\pi} \quad \text{as } x \rightarrow \infty , \quad (18)$$

so that (16) reduces to

$$\frac{\partial U_\Lambda(\varphi, T=0)}{\partial \Lambda} = -\frac{K_4}{2} \Lambda^3 \ln[\Lambda^2 + U_\Lambda''(\varphi)] \quad (19)$$

in the limit $T \rightarrow 0$. Comparison with (14) shows that this is indeed the correct zero temperature equation. It is also instructive to look at the opposite limit, $T \gg \Lambda$. Using $g(x) = x/2\pi$ for $x < 2\pi$ we obtain

$$\frac{\partial U_\Lambda(\varphi, T)}{\partial \Lambda} = -\frac{K_3}{2} T \Lambda^2 \ln[\Lambda^2 + U_\Lambda''(\varphi)] \quad \text{for } T \gg \Lambda. \quad (20)$$

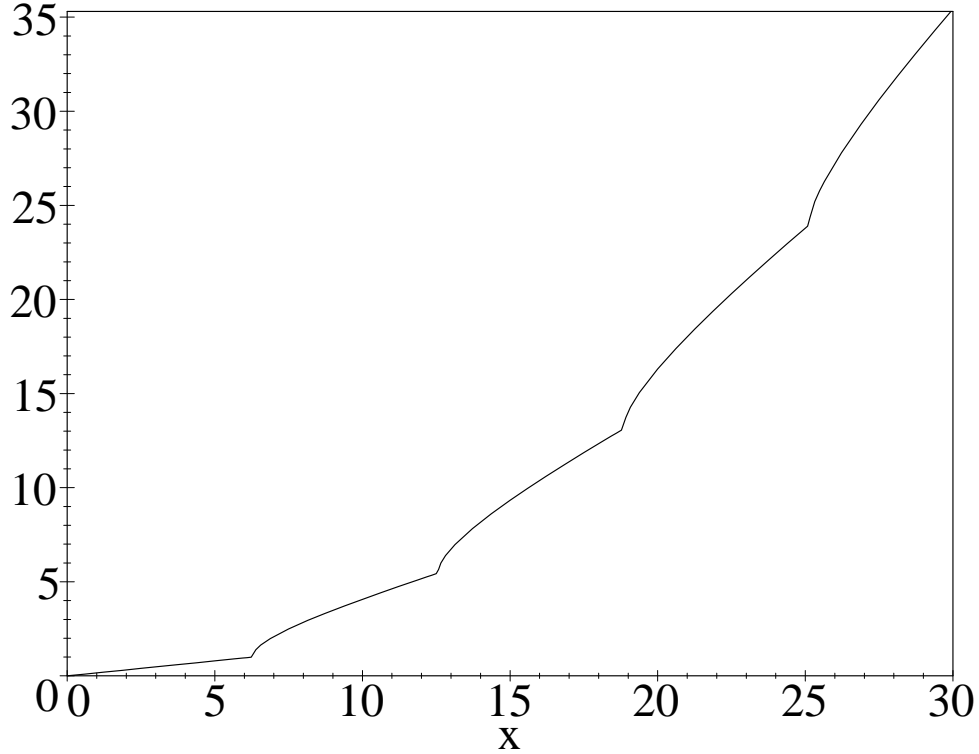


Figure 1: The function $g(x)$.

On comparing with (14) we see that this is simply T times the zero temperature flow equation for a three dimensional theory. Hence we already see evidence for dimensional reduction at high temperature.

For later use we record here the analog of (16) for theories involving multiple scalar fields. The generalization is entirely straight forward, the result being

$$\frac{\partial U_{\Lambda}(\varphi, T)}{\partial \Lambda} = -\frac{K_3}{2} 2\pi T^2 \Lambda g\left(\frac{\Lambda}{T}\right) \ln \det \left[\Lambda^2 + \frac{\partial^2 U_{\Lambda}(\varphi)}{\partial \varphi_i \partial \varphi_j} \right] \quad (21)$$

where $g(\Lambda/T)$ is given by (17) as before.

Before concluding this section we point out that there exists in the literature an alternative method of including finite temperature effects in the

sharp cutoff case [19]. It amounts to replacing q by $|\mathbf{q}|$ in the delta function of (15). The result is

$$\frac{\partial U_\Lambda(\varphi, T)}{\partial \Lambda} \propto \sum_{n=-\infty}^{\infty} \ln[\omega_n^2 + \Lambda^2 + U_\Lambda''(\varphi, T)] . \quad (22)$$

The sum over Matsubara frequencies may now be done analytically, and the resulting equation involves no dependence on n , in contrast to (16). However, by cutting off only the three momenta and summing over all n one is neglecting the effect of integrating out the Matsubara modes with $\omega_n > \Lambda$ on the effective potential. As noted following (14), it is precisely this kind of feedback that leads to the incorporation of higher loop effects. The equation derived from (22) has the additional unpleasant feature that it does not reduce to the zero temperature equation (14) in the limit $T \rightarrow 0$ [20].

3 $\lambda\varphi^4$ Theory

In this section we will discuss briefly the finite temperature phase transition for a simple \mathbb{Z}_2 symmetric scalar field theory. This model has already been analyzed using the Wilson RG approach [15, 20], and it is included here mainly to illustrate the method. It is worth noting, however, that the previous treatments differ from ours in the details of the implementation: [15] uses a smooth cutoff, and in [20] a sharp cutoff is used only for the three-momentum, as discussed in the last paragraph of the previous section.

Consider then a \mathbb{Z}_2 symmetric theory with Lagrangian

$$\mathcal{L} = \frac{1}{2} \partial_\mu \varphi \partial^\mu \varphi - V(\rho) , \quad (23)$$

where $\rho \equiv \frac{1}{2} \varphi^2$. Our RG equation for the effective potential (16) becomes

$$\frac{\partial U_\Lambda(\rho, T)}{\partial \Lambda} = -\frac{\Lambda T^2}{2\pi} g\left(\frac{\Lambda}{T}\right) \ln \left[\Lambda^2 + \frac{\partial U_\Lambda(\rho, T)}{\partial \rho} + 2\rho \frac{\partial^2 U_\Lambda(\rho, T)}{\partial \rho^2} \right] . \quad (24)$$

We wish to solve (24) subject to the boundary condition⁵ $U_{\Lambda_0}(\rho, T) = V(\rho)$. This is still rather difficult, and to make progress we expand U_Λ in a Taylor

⁵See (11). Note that consistency requires that we keep $T \ll \Lambda_0$ at all times.

series about its minimum. This leads to an infinite set of coupled nonlinear ordinary differential equations, which may be approximately solved by truncation.

Let us start with the symmetric regime, where the minimum of U_Λ is at the origin. We parameterize U_Λ in terms of its successive derivatives:

$$m^2(\Lambda, T) \equiv U_\Lambda^{(1)}(\rho = 0, T) , \quad (25)$$

$$\lambda_{2n}(\Lambda, T) \equiv \frac{1}{n!} U_\Lambda^{(n)}(\rho = 0, T) \quad \text{for } n \geq 2 , \quad (26)$$

where $U_\Lambda^{(n)} \equiv \frac{\partial^n U_\Lambda}{\partial \rho^n}$. Evolution equations for these parameters are easily derived by differentiating (24) with respect to ρ . The first three equations obtained in this way are:

$$\frac{dm^2}{d\Lambda} = -\frac{\Lambda T^2}{2\pi} g\left(\frac{\Lambda}{T}\right) \frac{6\lambda_4}{\Lambda^2 + m^2} , \quad (27)$$

$$\frac{d\lambda_4}{d\Lambda} = -\frac{\Lambda T^2}{2\pi} g\left(\frac{\Lambda}{T}\right) \left[\frac{15\lambda_6}{\Lambda^2 + m^2} - \frac{18\lambda_4^2}{(\Lambda^2 + m^2)^2} \right] , \quad (28)$$

$$\begin{aligned} \frac{d\lambda_6}{d\Lambda} = -\frac{\Lambda T^2}{2\pi} g\left(\frac{\Lambda}{T}\right) & \left[\frac{28\lambda_8}{\Lambda^2 + m^2} - \frac{90\lambda_6\lambda_4}{(\Lambda^2 + m^2)^2} \right. \\ & \left. + \frac{72\lambda_4^3}{(\Lambda^2 + m^2)^3} \right] . \end{aligned} \quad (29)$$

Several remarks are in order at this point. First, note that the above expressions have an obvious interpretation in terms of one-loop Feynman diagrams. For example, (28) says that the four point function receives contributions from the diagrams in Fig. 2. Figure 2(a) corresponds to the second

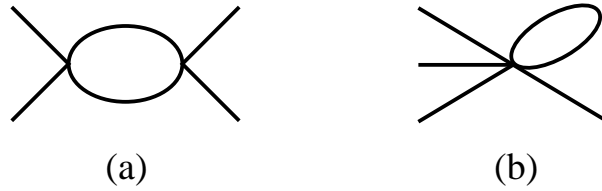


Figure 2: Contributions to the running of λ_4 .

term in square brackets of (28), which involves two 4-point couplings and two

“propagators”, while Fig. 2(b) corresponds to the first term in square brackets, involving the 6-point coupling and one “propagator”. The other flow equations can be given similar interpretations. We also see how integrating out the high frequency modes generates new local interactions: even if one starts with a φ^4 potential at Λ_0 , higher order terms are created as the cutoff is lowered. Finally note that the equations describe naturally how particles with mass larger than Λ “decouple”, in the sense that their effect on the running parameters becomes very small .

Now let us derive the flow equations in the broken regime, where the minimum of the potential is at some $\rho_0 > 0$. Here we parameterize U_Λ in terms of the location of its minimum and consecutive derivatives at that point. The flow equation for $\rho_0(\Lambda, T)$ is obtained from the condition

$$\frac{\partial U_\Lambda}{\partial \rho}(\rho_0, T) = 0 . \quad (30)$$

Taking the Λ derivative of (30) we obtain (primes denote derivatives with respect to ρ):

$$\frac{\partial U'_\Lambda}{\partial \Lambda} + U''_\Lambda \frac{d\rho_0}{d\Lambda} = 0 , \quad (31)$$

so that

$$\frac{d\rho_0}{d\Lambda} = -\frac{\partial U'_\Lambda}{\partial \Lambda} \frac{1}{U''_\Lambda} \quad (32)$$

(all U_Λ derivatives are evaluated at ρ_0 , of course). The other parameters are defined as in (26):

$$\lambda_{2n}(\Lambda, T) \equiv \frac{1}{n!} U_\Lambda^{(n)}(\rho_0, T) , \quad (33)$$

for $n \geq 2$. The flow equations for these parameters are obtained by differentiating (24) with respect to ρ and evaluating the result at ρ_0 . The first three are:

$$\frac{d\rho_0}{d\Lambda} = \frac{\Lambda T^2}{2\pi} g\left(\frac{\Lambda}{T}\right) \left[\frac{6\lambda_4 + 12\rho_0\lambda_6}{\Lambda^2 + 4\rho_0\lambda_4} \right] \frac{1}{2\lambda_4} , \quad (34)$$

$$\frac{d\lambda_4}{d\Lambda} = -\frac{\Lambda T^2}{2\pi} g\left(\frac{\Lambda}{T}\right) \left[\frac{15\lambda_6 + 24\rho_0\lambda_8}{\Lambda^2 + 4\rho_0\lambda_4} - \frac{(6\lambda_4 + 12\rho_0\lambda_6)^2}{2(\Lambda^2 + 4\rho_0\lambda_4)^2} \right] + 3\lambda_6 \frac{d\rho_0}{d\Lambda} , \quad (35)$$

$$\begin{aligned} \frac{d\lambda_6}{d\Lambda} = & -\frac{\Lambda T^2}{2\pi} g\left(\frac{\Lambda}{T}\right) \left[\frac{28\lambda_8 + 40\rho_0\lambda_{10}}{\Lambda^2 + 4\rho_0\lambda_4} - \frac{(15\lambda_6 + 24\rho_0\lambda_8)(6\lambda_4 + 12\rho_0\lambda_6)}{(\Lambda^2 + 4\rho_0\lambda_4)^2} \right. \\ & \left. + \frac{(6\lambda_4 + 12\rho_0\lambda_6)^3}{3(\Lambda^2 + 4\rho_0\lambda_4)^3} \right] + 4\lambda_8 \frac{d\rho_0}{d\Lambda}. \end{aligned} \quad (36)$$

We begin our study of the high temperature phase transition by computing the effective potential in the simplest possible approximation. This amounts to parameterizing U_Λ in terms of its first two derivatives only, i.e., we set $\lambda_n = 0$ for $n \geq 6$. Our strategy is then as follows: we define the theory by specifying “renormalized” zero temperature parameters at $\Lambda = T = 0$. We may choose the zero temperature theory to be in the symmetric regime by picking $m_r^2 \equiv m^2(0,0) > 0$ or in the broken regime by picking $\rho_{0r} \equiv \rho_0(0,0) > 0$. Depending on the chosen phase, we then use either (27),(28) or (34),(35) to numerically integrate up in Λ to some $\Lambda_0 \gg m_r$ or $\sqrt{\rho_{0r}}$. This “integrating up” is done at $T = 0$, and it serves merely to provide us with the “bare” parameters that define the action S_{Λ_0} . We note that if m^2 or ρ_0 go to zero at some intermediate $\tilde{\Lambda}$, then we continue the integration with the set of equations appropriate to the new phase, taking the values of the parameters at $\tilde{\Lambda}$ as initial conditions.

With the parameters at Λ_0 in hand we are now ready to study the effects of finite temperature. This is done by fixing $T \neq 0$ in the evolution equations and running down from Λ_0 to $\Lambda = 0$. Repeating this for different values of T allows one to determine the temperature dependence of the renormalized parameters. Figures 3 and 4 show the evolution in Λ of the parameters at various temperatures. The initial conditions are such that the zero temperature theory is in the broken phase. From Fig. 3 we see that ρ_0 is quadratically renormalized for large Λ and approaches a constant as $\Lambda \rightarrow 0$. As the temperature is increased, the asymptotic value of ρ_0 decreases, until at T_c we have $\rho_0(\Lambda, T_c) \rightarrow 0$ as $\Lambda \rightarrow 0$. Above T_c ρ_0 goes to zero for finite Λ , and we continue the evolution in the symmetric regime. Figure 4 shows the corresponding behavior of λ_4 . At $T = 0$ we observe the expected logarithmic evolution. Above and below T_c , where all modes are massive, the running of λ_4 is effectively stopped when Λ becomes much smaller than the relevant mass scale. At T_c , however, λ_4 runs to zero. This is, in fact, expected, because at the critical temperature the theory is scale invariant and the phase transition is second order. As a consequence the parameters run according to their canonical dimension, which is one for λ_4 at small Λ since

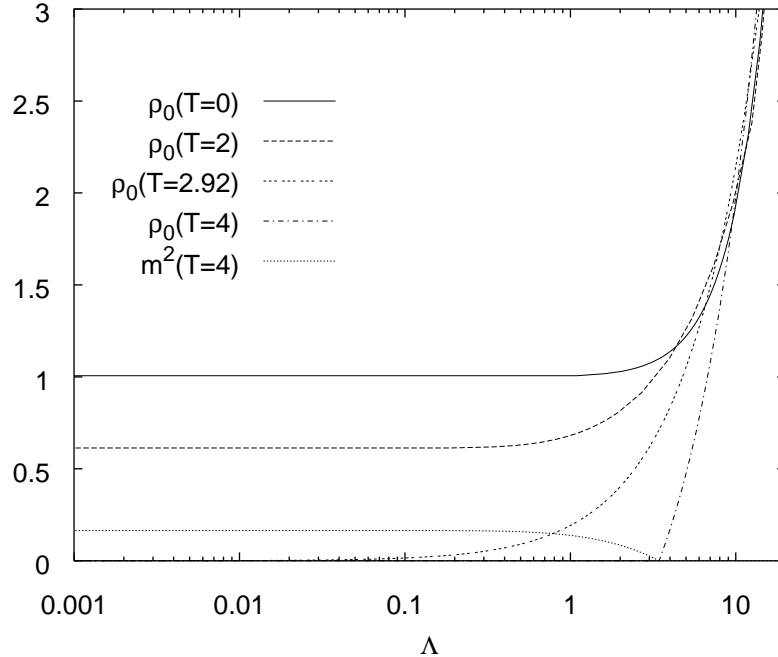


Figure 3: The evolution of ρ_0 at various temperatures. For $T > T_c$, the running of the mass term in the symmetric regime is also shown.

to the long wavelength modes the theory looks effectively three dimensional at high temperature⁶. It is the fact that the Wilson RG approach correctly takes into account the strong renormalization of the coupling in the vicinity of the phase transition that allows one to accurately describe the physics in this region, including critical exponents [14, 15, 17]. This is to be contrasted with the loop expansion, where higher order terms go like $\lambda_4 T/\mathcal{M}$ to some power, with \mathcal{M} the appropriate infrared cutoff. Since $\mathcal{M} \rightarrow 0$ at T_c , the expansion necessarily breaks down near the phase transition.

Figure 5 shows the temperature dependence of the “renormalized” (i.e. $\Lambda = 0$) parameters. The critical temperature is given by $T_c^2/\rho_{0r} \approx 8.60$, whereas naive one-loop perturbation theory predicts $T_c^2/\rho_{0r} = 8$ [2, 3]. In light of the fact that the loop expansion breaks down near the phase transition this good agreement may seem surprising, but it is in fact expected:

⁶This is explained in more detail in the appendix.

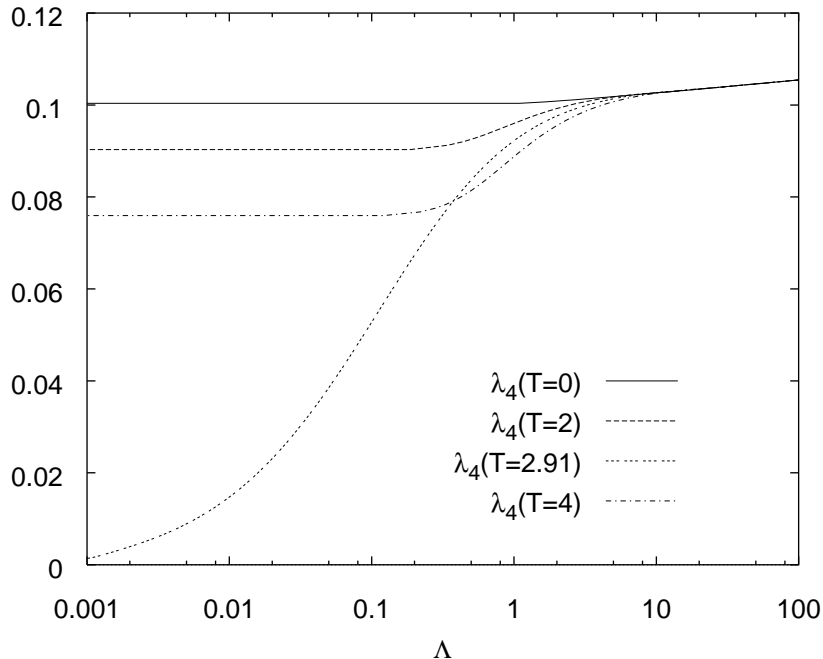


Figure 4: The evolution of λ_4 at various temperatures.

since perturbation theory is valid both far above and far below⁷ the critical temperature, one can show that the error in the naive value of T_c is of order $\lambda_4 T_c$ [2]. The above results may also be compared with [15], where finite temperature φ^4 theory was treated using a smooth cutoff flow equation.

Before going on to theories involving multiple scalar fields a discussion of the validity of our approximation method is in order. We will not comment on the initial step of obtaining (14) from (7) by discarding the momentum dependence; for this we refer the reader to the literature [10, 21, 18]. What we do want to address is the effect of truncating the infinite set of coupled differential equations. Instead of discussing the formal aspects of the problem (see for example [11, 18]), we will focus on a simple practical test: if the truncation is to be sensible at all, then the effect of including additional terms must be, in some sense, “small”.

To see if this is the case we derived flow equations analogous to (27)–(29)

⁷As long as there are no Goldstone modes.

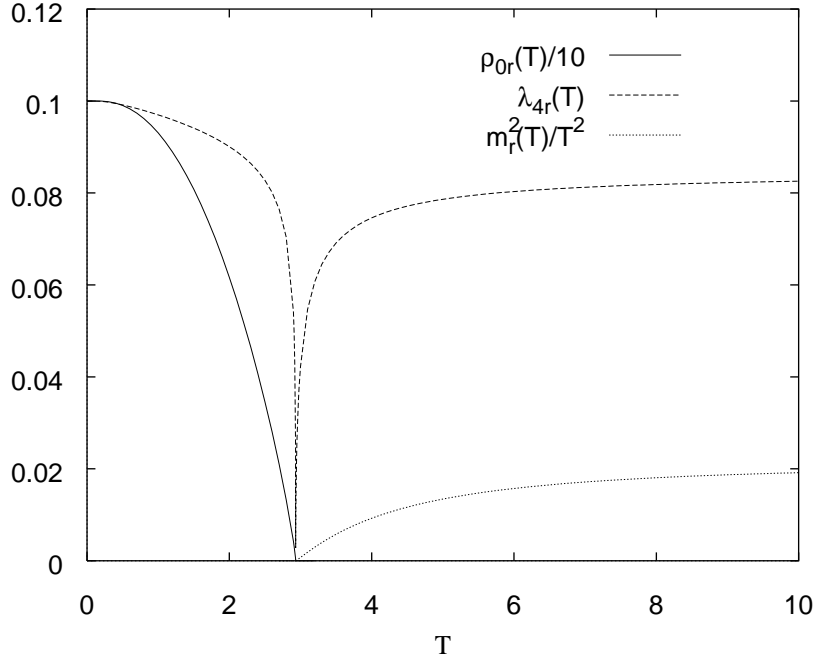


Figure 5: The temperature dependence of the renormalized parameters.

and (34)–(36) up to and including λ_{14} . Solving this set of seven coupled equations requires a change in tactics. Recall that before we were able to specify the renormalized ($\Lambda = 0$) parameters and then integrate up to obtain the “bare” parameters at Λ_0 . This is no longer possible, because the newly included couplings λ_6 – λ_{14} correspond to irrelevant operators. This means that their values in the infrared are fixed in terms of the values of the relevant parameters m^2 and λ_4 , and consequently they may not be chosen independently [22].

To isolate the effect of including the additional terms we therefore proceed as follows. Start at Λ_0 and set λ_6 – λ_{14} arbitrarily to zero⁸. Then fine tune $\rho_0(\Lambda_0)$ and $\lambda_4(\Lambda_0)$ until flowing to the infrared produces $\rho_{0r} = \rho_0(\Lambda = 0) = 1$ and $\lambda_{4r} = \lambda_4(\Lambda = 0) = 0.1$. At this point we know we are dealing with the same theory as before, and we may now switch on the temperature and find T_c . This procedure was carried out for several different values of λ_4 ,

⁸Any other “natural” value would do just as well, where “natural” means $\mathcal{O}(1)$ divided by enough powers of Λ_0 to get the dimension right.

Table 1: T_c^2/ρ_{0r} for various approximation methods and coupling values.

Calculation Method	λ_{4r}		
	0.01	0.1	1.0
1-loop Pert. Th.	8	8	8
Wilson RG up to λ_4	8.29	8.60	10.37
Wilson RG up to λ_{14}	8.28	8.55	9.69

the results being summarized in table 1. We see that at least for moderate couplings the effect of including parameters beyond λ_4 is small. This is in accord with the expectation that as long as the effective potential is not too steep the first two terms in the Taylor expansion should accurately describe its shape around the minimum.

4 Inverse Symmetry Breaking

The simplest model that exhibits an inverse phase structure is a $\mathbb{Z}_2 \times \mathbb{Z}_2$ symmetric scalar field theory described by the Lagrangian

$$\mathcal{L} = \frac{1}{2}(\partial_\mu \varphi)^2 + \frac{1}{2}(\partial_\mu \chi)^2 - V(\varphi, \chi) , \quad (37)$$

where

$$V(\varphi, \chi) = \frac{1}{2}m^2\varphi^2 + \frac{1}{2}\mu^2\chi^2 + \frac{\lambda_\varphi}{4}\varphi^4 + \frac{\lambda_\chi}{4}\chi^4 - \frac{\lambda_{\varphi\chi}}{2}\varphi^2\chi^2. \quad (38)$$

Note that, if the λ 's are all positive, we require

$$\lambda_\varphi\lambda_\chi > \lambda_{\varphi\chi}^2 \quad (39)$$

for boundedness. If one calculates the finite temperature effective potential for this theory to one loop and then expands the result about the origin one finds that the quadratic part at high temperature is

$$\begin{aligned} V_{1\text{-loop}}^{\text{quad}} &= \frac{1}{2} \left(m^2 + \frac{T^2}{12}(3\lambda_\varphi - \lambda_{\varphi\chi}) \right) \varphi^2 \\ &+ \frac{1}{2} \left(\mu^2 + \frac{T^2}{12}(3\lambda_\chi - \lambda_{\varphi\chi}) \right) \chi^2 . \end{aligned} \quad (40)$$

It is easy to see that this form allows a myriad of different symmetry breaking patterns. Depending on the relative size of the couplings and the signs of m^2 and μ^2 , one can have symmetry breaking, restoration, or non-restoration at high temperature. Although less obvious, there are even more exotic possibilities: for example, one can have a symmetry broken or restored only for an intermediate range of temperatures [23].

Let us now analyze this model using the Wilson RG formalism developed in the previous section. Because of the $\mathbb{Z}_2 \times \mathbb{Z}_2$ invariance the Lagrangian may be written as

$$\mathcal{L} = \frac{1}{2}(\partial_\mu \varphi)^2 + \frac{1}{2}(\partial_\mu \chi)^2 - V(\rho, \zeta) , \quad (41)$$

where

$$\rho \equiv \frac{1}{2}\varphi^2 \quad (42)$$

and

$$\zeta \equiv \frac{1}{2}\chi^2 . \quad (43)$$

We proceed as in the previous section. The RG equation (21) for this model is

$$\frac{\partial U_\Lambda(\rho, \zeta, T)}{\partial \Lambda} = -\frac{K_3}{2} 2\pi T^2 \Lambda g \left(\frac{\Lambda}{T} \right) \ln \det \mathcal{M} , \quad (44)$$

where

$$\mathcal{M} = \begin{bmatrix} \Lambda^2 + \frac{\partial U_\Lambda}{\partial \rho} + 2\rho \frac{\partial^2 U_\Lambda}{\partial \rho^2} & 2\rho^{\frac{1}{2}} \zeta^{\frac{1}{2}} \frac{\partial^2 U}{\partial \rho \partial \zeta} \\ 2\rho^{\frac{1}{2}} \zeta^{\frac{1}{2}} \frac{\partial^2 U}{\partial \rho \partial \zeta} & \Lambda^2 + \frac{\partial U_\Lambda}{\partial \zeta} + 2\zeta \frac{\partial^2 U_\Lambda}{\partial \zeta^2} \end{bmatrix} . \quad (45)$$

The potential U_Λ is again parameterized by its first two derivatives at the minimum, but this time we must distinguish four cases: the minimum may lie at the origin, on either axis, or between the axes. In all four cases the couplings are defined via

$$\lambda_\varphi(\Lambda, T) \equiv \left. \frac{1}{2} \frac{\partial^2 U_\Lambda(T)}{\partial \rho^2} \right|_{\min} , \quad (46)$$

$$\lambda_\chi(\Lambda, T) \equiv \left. \frac{1}{2} \frac{\partial^2 U_\Lambda(T)}{\partial \zeta^2} \right|_{\min} , \quad (47)$$

$$\lambda_{\varphi\chi}(\Lambda, T) \equiv -\left. \frac{1}{2} \frac{\partial^2 U_\Lambda(T)}{\partial \rho \partial \zeta} \right|_{\min} . \quad (48)$$

The other two parameters used to describe the potential depend on the location of the minimum. If it is at the origin, we simply define

$$m^2(\Lambda, T) \equiv \frac{\partial U_\Lambda(0, 0, T)}{\partial \rho} , \quad (49)$$

$$\mu^2(\Lambda, T) \equiv \frac{\partial U_\Lambda(0, 0, T)}{\partial \zeta} . \quad (50)$$

If the minimum is at ρ_0 on the ρ axis, we use

$$\mu^2(\Lambda, T) \equiv \frac{\partial U_\Lambda(\rho_0, 0, T)}{\partial \zeta} \quad (51)$$

and ρ_0 to parameterize U_Λ . The flow equation for ρ_0 is derived as in (30)–(32). Similarly, if the minimum is on the ζ axis,

$$m^2(\Lambda, T) \equiv \frac{\partial U_\Lambda(0, \zeta_0, T)}{\partial \rho} \quad (52)$$

and ζ_0 are used. The final possibility is that the minimum lies between the axes. In this case we parameterize in terms of its location in field space, (ρ_0, ζ_0) . The flow equations for these coordinates are obtained by taking total Λ derivatives of the two expressions

$$\frac{\partial U_\Lambda(\rho_0, \zeta_0)}{\partial \rho} = 0 \quad (53)$$

and

$$\frac{\partial U_\Lambda(\rho_0, \zeta_0)}{\partial \zeta} = 0 . \quad (54)$$

This yields two simultaneous algebraic equations for $d\rho_0/d\Lambda$ and $d\zeta_0/d\Lambda$, which may be solved to give

$$\frac{d\rho_0}{d\Lambda} = -\frac{1}{2} \frac{\lambda_\chi \frac{\partial}{\partial \rho} \left(\frac{\partial U_\Lambda}{\partial \Lambda} \right) \Big|_{(\rho_0, \zeta_0)} + \lambda_{\varphi\chi} \frac{\partial}{\partial \zeta} \left(\frac{\partial U_\Lambda}{\partial \Lambda} \right) \Big|_{(\rho_0, \zeta_0)}}{\lambda_\varphi \lambda_\chi - \lambda_{\varphi\chi}^2} , \quad (55)$$

$$\frac{d\zeta_0}{d\Lambda} = -\frac{1}{2} \frac{\lambda_\varphi \frac{\partial}{\partial \zeta} \left(\frac{\partial U_\Lambda}{\partial \Lambda} \right) \Big|_{(\rho_0, \zeta_0)} + \lambda_{\varphi\chi} \frac{\partial}{\partial \rho} \left(\frac{\partial U_\Lambda}{\partial \Lambda} \right) \Big|_{(\rho_0, \zeta_0)}}{\lambda_\varphi \lambda_\chi - \lambda_{\varphi\chi}^2} . \quad (56)$$

As before, the right hand sides of the evolution equations are expressed in terms of our parameters by differentiating (44) with respect to the fields, evaluating the result at the appropriate minimum, and then dropping all terms with three or more derivatives. For example, the flow equations for the symmetric regime (i.e. minimum at the origin) are as follows:

$$\frac{dm^2}{d\Lambda} = -\frac{\Lambda T^2}{2\pi} g\left(\frac{\Lambda}{T}\right) \left[\frac{6\lambda_\varphi}{\Lambda^2 + m^2} - \frac{2\lambda_{\varphi\chi}}{\Lambda^2 + \mu^2} \right], \quad (57)$$

$$\frac{d\mu^2}{d\Lambda} = -\frac{\Lambda T^2}{2\pi} g\left(\frac{\Lambda}{T}\right) \left[\frac{6\lambda_\chi}{\Lambda^2 + \mu^2} - \frac{2\lambda_{\varphi\chi}}{\Lambda^2 + m^2} \right], \quad (58)$$

$$\frac{d\lambda_\varphi}{d\Lambda} = \frac{\Lambda T^2}{2\pi} g\left(\frac{\Lambda}{T}\right) \left[\frac{18\lambda_\varphi^2}{(\Lambda^2 + m^2)^2} + \frac{2\lambda_{\varphi\chi}^2}{(\Lambda^2 + \mu^2)^2} \right], \quad (59)$$

$$\frac{d\lambda_\chi}{d\Lambda} = \frac{\Lambda T^2}{2\pi} g\left(\frac{\Lambda}{T}\right) \left[\frac{18\lambda_\chi^2}{(\Lambda^2 + \mu^2)^2} + \frac{2\lambda_{\varphi\chi}^2}{(\Lambda^2 + m^2)^2} \right], \quad (60)$$

$$\begin{aligned} \frac{d\lambda_{\varphi\chi}}{d\Lambda} = \frac{\Lambda T^2}{2\pi} g\left(\frac{\Lambda}{T}\right) & \left[\frac{6\lambda_\varphi\lambda_{\varphi\chi}}{(\Lambda^2 + m^2)^2} + \frac{6\lambda_\chi\lambda_{\varphi\chi}}{(\Lambda^2 + \mu^2)^2} \right. \\ & \left. - \frac{8\lambda_{\varphi\chi}^2}{(\Lambda^2 + m^2)(\Lambda^2 + \mu^2)} \right]. \end{aligned} \quad (61)$$

There are similar, albeit more complicated, sets of equations for the other three positions of the minimum.

We begin our numerical study of the model by investigating the phenomenon of inverse symmetry breaking. By this we mean choosing the parameters so that the vacuum is symmetric at $T = 0$ but asymmetric at high temperature. From (40) it is clear that according to the one-loop result this happens if, say, $\lambda_{\varphi\chi} > 3\lambda_\varphi$ ⁹. The critical temperature is predicted to be

$$\frac{T_c^2}{m^2} = \frac{12}{\lambda_{\varphi\chi} - 3\lambda_\varphi}, \quad (62)$$

independent of λ_χ and μ^2 .

The flow equations are solved as in the previous section. Renormalized parameters are chosen at $T = \Lambda = 0$ in such a way that the vacuum is symmetric. The equations are then integrated to some Λ_0 much larger than all

⁹ (39) then requires that $\lambda_\chi > \lambda_{\varphi\chi}$, so the other symmetry cannot be broken at high T .

physical masses. Since the minimum moves away from the origin during this process it was necessary to develop an algorithm that automatically switches to the correct set of equations depending on the location of the minimum. Once the parameters at Λ_0 are known the temperature is switched on and the equations are integrated back down to $\Lambda = 0$, yielding the renormalized finite temperature values for the masses, vacuum expectation values, and couplings.

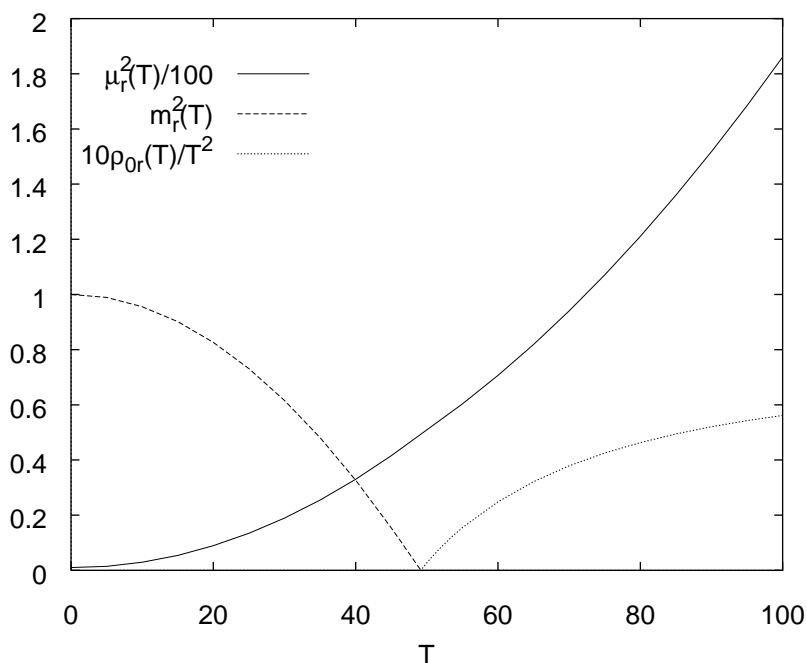


Figure 6: The masses and ρ_{0r} as a function of temperature.

Figures 6 and 7 show the behavior of the renormalized parameters for a typical case. The parameters are chosen so that naively (i.e. according to (40)) the \mathbb{Z}_2 symmetry of the φ -field is broken at high temperature. From Fig. 6 we see that this picture is confirmed by our RG approach. As the temperature increases $m_r^2(T)$ decreases and eventually hits zero at $T_c \approx 49$. Both $\mu_r^2(T)$ and $\rho_{0r}(T)$ are proportional to T^2 at high temperature. Figure 7 shows the corresponding behavior of the couplings. As in the φ^4 case discussed in the previous section, there is dramatic renormalization in the

vicinity of the phase transition¹⁰.

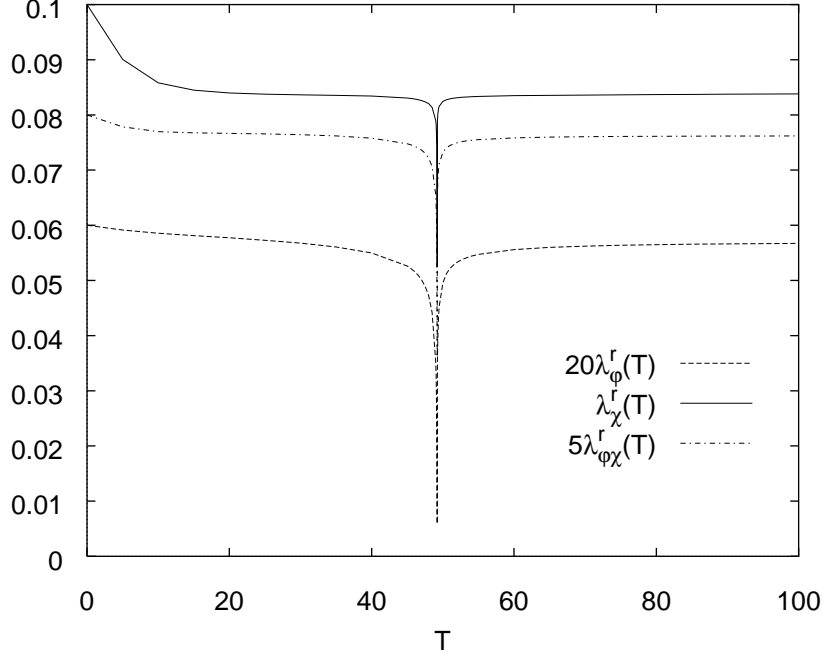


Figure 7: The couplings as a function of temperature.

Figure 8 compares the numerical value of the critical temperature with the naive prediction, equation (62), for several values of the cross-coupling. Even for the relatively small couplings chosen there are significant differences for all values of $\lambda_{\varphi\chi}^r$. The best agreement occurs for large values of $\lambda_{\varphi\chi}^r$, but even here the difference is about 15%. (Note that (39) requires that $\lambda_{\varphi\chi}^r < 0.0173$. Numerically the system becomes unstable slightly later, at $\lambda_{\varphi\chi}^r \approx 0.018$.) As $\lambda_{\varphi\chi}^r$ decreases, the deviation between the naive prediction and the numerical result increases rapidly. For $\lambda_{\varphi\chi}^r = 0.0105$, the difference is more than a factor two. For $\lambda_{\varphi\chi}^r = 0.01$, perturbation theory predicts $T_c/m_r \approx 109$. The numerical solution shows that there is no phase transition at all for these values of the parameters, and that $m_r^2(T)$ is in fact an increasing function of T at high temperature.

That the RG calculation gives a significantly higher critical temperature

¹⁰The behavior of the couplings near T_c is discussed in more detail in the appendix.

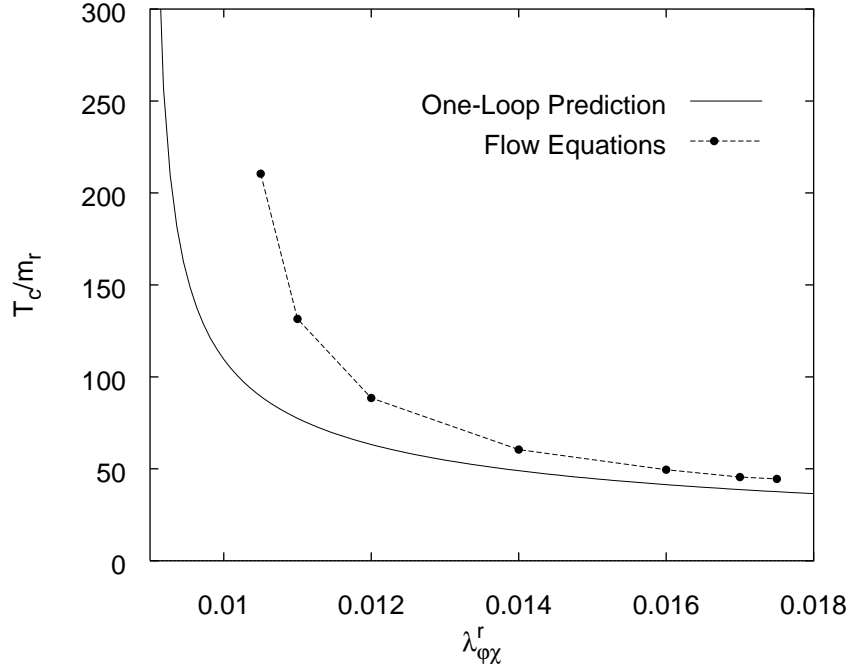


Figure 8: Comparing the critical temperature obtained from one-loop perturbation theory with that obtained by integrating the RG equations. ($\lambda_\varphi^r = 0.003$, $\lambda_\chi^r = 0.1$, $\mu_r^2 = 1$)

than perturbation theory is due to a combination of two factors. First of all, the renormalized couplings decrease with temperature, which raises T_c . This effect, however, is also present in the simple φ^4 case, and as was shown in section 3, there the two methods agree quite well. It alone therefore cannot account for the difference in critical temperatures. In fact, the dominant reason for the discrepancy is most easily seen in Eq. (57). The “propagator” in the second term is $\Lambda^2 + \mu^2$, and μ^2 is a rapidly increasing function of temperature. Hence at high T the second term is suppressed compared to the first, which significantly diminishes the effect of the cross-coupling $\lambda_{\phi\chi}$, and consequently raises T_c .

We have just seen that the temperature dependence of μ^2 plays an important role in determining T_c . Since the leading correction to μ^2 is proportional to λ_χ we may therefore suspect that the critical temperature also depends on the value of this coupling, even though the one-loop result (62) predicts that

it does not. The question is settled by Fig. 9, which shows the dependence of T_c on λ_χ . The effect is clearly quite large and increases rapidly as the coupling increases. Note that $\lambda_\chi > 0.0521$ is required for boundedness.

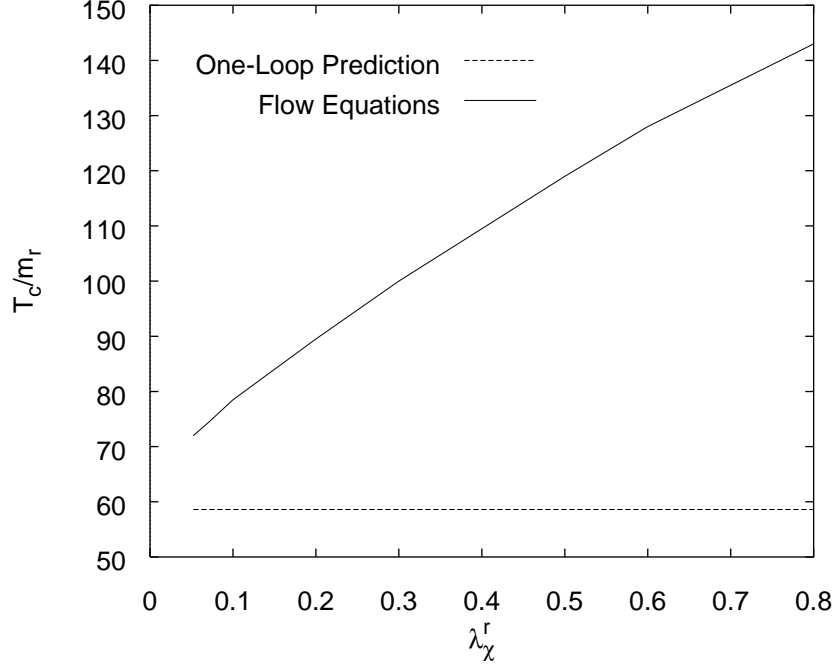


Figure 9: The dependence of the critical temperature on λ_χ^r . ($\lambda_\varphi^r = 0.003$, $\lambda_{\varphi\chi}^r = 0.0125$, $\mu_r^2 = 1$)

Figures 8 and 9 indicate that the critical temperatures obtained from the RG approach are consistently higher than those gotten from the loop expansion, and that certain sets of couplings don't produce a phase transition at all even though $\lambda_{\varphi\chi} > 3\lambda_\varphi$. This may lead one to the conclusion that the region of parameter space which yields an inverse phase structure is significantly smaller than that predicted by the one-loop result. We emphasize that this is not the case. The reason is again the presence of the “propagators” in the flow equations. As explained above, for the case at hand these factors reduce the significance of the $\lambda_{\varphi\chi}$ term, which raises T_c and suppresses the phase transition. But at the same time the suppression of $\lambda_{\varphi\chi}$ tends to stabilize the system, which means that there is additional parameter space beyond

Table 2: T_c/m_r for various approximation methods and couplings ($\mu_r^2 \approx 1$ in all cases). “Up to dim. n” means that operators of dimension higher than n were discarded in the flow equations.

$\lambda_\varphi^r =$	2.78×10^{-3}	1×10^{-2}	1×10^{-4}
$\lambda_\chi^r =$	1.00×10^{-1}	3×10^{-1}	3×10^{-3}
$\lambda_{\varphi\chi}^r =$	1.25×10^{-2}	5×10^{-2}	5×10^{-4}
1-loop Pert. Theory	53.7	24.5	245
RG up to dim. 4 ops.	67.9	33.6	257
RG up to dim. 8 ops.	67.9	33.5	257

the limit (39) for which transitions occur. The net effect is then a shift of the inverse-breaking region rather than a major reduction.

To make sure that the numerical results do not depend significantly on the order of truncation of the evolution equations it is necessary to study the effect of including higher dimensional operators. To this end we enlarged our system of equations to include the couplings corresponding to operators of dimension less than or equal to eight, e.g., φ^8 , $\varphi^2\chi^4$, χ^6 , etc. This results in a system of sixteen coupled first order nonlinear differential equations. As discussed at the end of section 3, the addition of irrelevant operators causes the complication that one can no longer simply choose the renormalized parameters. Instead, one must fine-tune the bare parameters at Λ_0 to achieve the desired values for the masses and relevant couplings in the infrared. Aside from this nuisance the solution of the equations proceeds as before. The results are summarized in table 2, which shows that the effect of the added terms is very small. We conclude that discarding operators of mass dimension higher than four is a valid approximation for the purpose at hand. Table 2 also shows that for very small values of the couplings the numerical result is in reasonable agreement with the one-loop prediction, at least if $\lambda_{\varphi\chi}$ is safely larger than $3\lambda_\varphi$. For the couplings in column 2 the two methods differ by almost 40%, while the discrepancy is down to 5% for the values in column three.

5 The Coupling Constants at High Temperature

In this section we discuss the temperature dependence of the coupling constants in the high T limit. We begin with the simplest case, that of a single scalar field.

5.1 $\lambda\varphi^4$ Theory

The high temperature behavior of the quartic coupling λ has been the subject of controversy for some time. Several authors have found λ decreasing with T [24], others find λ approaching a constant as $T \rightarrow \infty$ [25], and still others find that λ is increasing at high temperature [26].

In order to shed some light on the issue we integrated the RG equations discussed in section 3 for a wide range of temperatures. The results are shown in Fig. 10. We see that the coupling constant rapidly decreases at first, but eventually turns around. From $T \approx 40$ onwards the dependence is clearly approximately logarithmic. We note that at least qualitatively this behavior agrees with that obtained in [27].

In the literature one frequently encounters the notion that the effect of high temperature on coupling constants may be incorporated by “running” the couplings according to their one-loop β -functions using the temperature as the scale [28]. In our case this amounts to assuming

$$\frac{d\lambda_{4r}}{dt} = \frac{9}{8\pi^2} \lambda_{4r}^2, \quad (63)$$

where $t = \ln(T/T_0)$, so that

$$\lambda_{4r}(T) = \frac{\lambda_{4r}(T_0)}{1 - \frac{9}{8\pi^2} \lambda_{4r}(T_0) \ln(T/T_0)}. \quad (64)$$

The justification for this procedure is usually based on rather vague arguments concerning the average momentum transfer during collisions of particles in the heat bath being $\mathcal{O}(T)$, so that a coupling constant at that scale ought to be appropriate. While this is certainly not unreasonable it is hardly a convincing argument, and as noted above a more detailed analysis has produced many other types of behavior. To see how well Eq. (63) describes

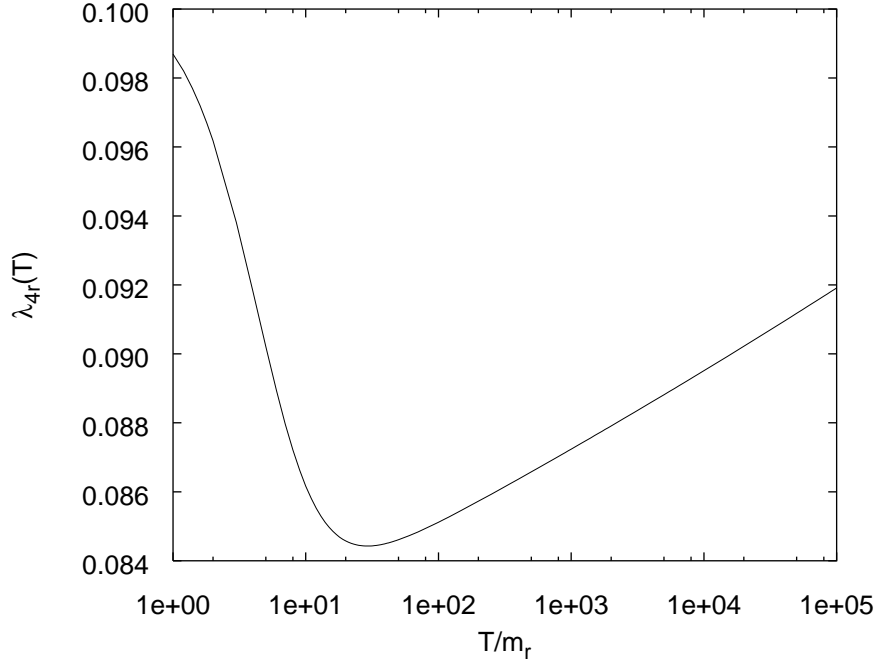


Figure 10: Temperature dependence of the quartic coupling constant. Note the logarithmic scale on the temperature axis. ($\lambda_{4r} = 0.1$)

the high temperature evolution we have plotted Eq. (64) together with the numerical integration in Fig. 11. The one-loop result is normalized so that the two methods agree at $T/m_r = 100$. It is clear from the figure that the high temperature dependence of $\lambda_{4r}(T)$ is described quite well by the one-loop β -function. After running T over three orders of magnitude the results differ by about 1.5%. It is also clear, however, that the difference becomes significant if one runs over many orders of magnitude, for example to the GUT scale. In addition we see that using the one-loop equation is only reasonable if one knows the correct “initial condition” at high temperature, in our case $\lambda_{4r}(T) \approx 0.085$ at $T/m_r = 100$. Starting the evolution using Eq. (64) with $\lambda_{4r}(T = 1) = 0.1$ is obviously not satisfactory, and obtaining the proper initial condition requires an analysis such as the one presented in this paper.

It is worthwhile noting that the general features of the high temperature behavior of the coupling can be understood by simply looking at its RG

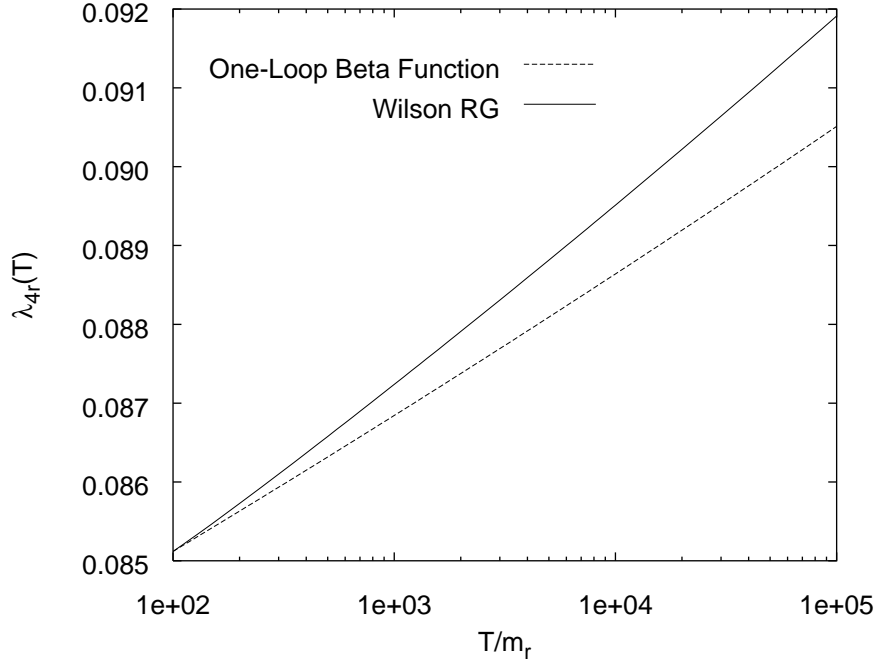


Figure 11: The high temperature evolution of $\lambda_{4r}(T)$ obtained from the RG compared to the behavior obtained by using T as the scale in the usual one-loop β -function. The initial condition for the one-loop integration is chosen so that the two methods agree at $T=100$. ($\lambda_{4r} = 0.1$)

equation, obtained in section 3. For $\lambda_6 = 0$ and $\Lambda \gg T$ and $|m|$, Eq. (28) reduces to Eq. (63). Thus the evolution for very large Λ is simply given by the one-loop β -function. Now for $T \gg m_r$ the propagator in (28) contains a large thermal mass, which means that the running effectively stops for $\Lambda < \sqrt{\lambda_4}T$. The evolution for $\Lambda \ll T$ is thus strongly suppressed, and all that remains is the one-loop-like running for large Λ plus some threshold effect for $\Lambda \sim T$. At a higher temperature the thermal mass is larger, causing the running of λ_4 to freeze out at larger Λ . The contribution from the threshold region is approximately the same as before, and so the net effect of increasing T from T_1 to T_2 is essentially equivalent to integrating the one-loop β -function between the two temperatures. This explains the correspondence in Fig. 11. The slope of the numerical curve is slightly steeper because the quantum corrections to the mass go like $-\lambda_4\Lambda^2$, which reduces the denominator in

(28) and makes λ_4 flow somewhat faster for large Λ than predicted by Eq. (63).

Having just explained why $\lambda_{4r}(T)$ should increase with temperature we find ourselves having to account for the initial decrease seen in Fig. 10. This decrease occurs for values of the temperature low enough so that the suppression of the evolution due to the thermal mass is not yet important. Instead the running is dominated by the range $\Lambda < T$, where the prefactor on the RHS of Eq. (28), $\Lambda T^2 g(\Lambda/T)$, is a rapidly increasing function of T . Thus, for moderate values of T , the coupling runs faster at higher temperature, which explains the initial decrease in $\lambda_{4r}(T)$.

We end this section with a few remarks. First of all, we have checked that the high temperature behavior of the coupling is not altered by the inclusion of higher dimensional operators in the flow equations. In fact, the effect of these operators decreases rapidly as one gets further away from the critical theory. Second, we point out that the author of [27], using an “improved” loop expansion approach, has found the high temperature evolution of the coupling to be similar to ours, i.e., approximately as predicted by the one-loop β -function with some temperature dependent correction. Finally, note that the calculations in this section were done for a theory that is symmetric at $T = 0$. This choice has no effect on the high temperature behavior of the coupling, for at very high T the theory does not care whether or not there was a phase transition at much lower temperature¹¹. For the temperature dependence of the coupling constant in an initially broken theory at moderate values of T see section 3.

5.2 $\mathbb{Z}_2 \times \mathbb{Z}_2$ Model

We will now study the high temperature behavior of the coupling constants of the $\mathbb{Z}_2 \times \mathbb{Z}_2$ model discussed in section 4. There are two possible phases at high temperature: either the theory is completely symmetric, or one of the two symmetries is broken. We have checked that in both cases for generic values of the zero temperature parameters the evolution of the couplings at high temperature is approximately given by their one-loop β -functions, viz.,

$$\frac{d\lambda_\varphi}{dt} = \frac{1}{8\pi^2} [9\lambda_\varphi^2 + \lambda_{\varphi\chi}^2], \quad (65)$$

¹¹This was also checked numerically.

$$\frac{d\lambda_\chi}{dt} = \frac{1}{8\pi^2}[9\lambda_\chi^2 + \lambda_{\varphi\chi}^2], \quad (66)$$

$$\frac{d\lambda_{\varphi\chi}}{dt} = \frac{1}{8\pi^2}[3(\lambda_\varphi + \lambda_\chi)\lambda_{\varphi\chi} - 4\lambda_{\varphi\chi}^2], \quad (67)$$

where $t = \ln(T/T_0)$. The reason for this behavior is essentially the same as in the φ^4 case discussed above, except that the situation is complicated by the presence of multiple mass scales. An example of the evolution of the

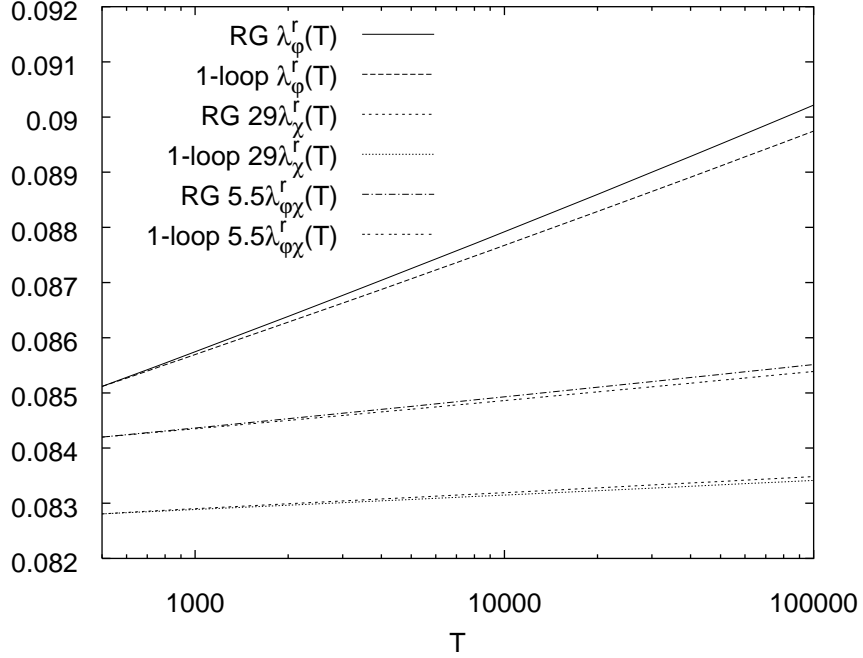


Figure 12: The high temperature evolution of the couplings. “RG” refers to the Wilson RG approach of this paper while “1-loop” refers to the numerical solution of equations (65)–(67). The initial conditions for the one-loop integration are chosen so that the two approaches agree at $T = 500$. ($m_r^2 = \mu_r^2 = 1$, $\lambda_\varphi^r = 0.1$, $\lambda_\chi^r = 0.003$, $\lambda_{\varphi\chi}^r = 0.016$)

couplings is shown in Fig. 12, which also presents the running according to the one-loop β -functions for comparison. We see that at least over the limited temperature range presented the two methods agree reasonably well. Note that the renormalized couplings in Fig. 12 are chosen so that the theory is

symmetric at $T = 0$ but broken at high temperature. The transition to the broken phase occurs at $T_c \approx 50$.

We conclude this section by discussing an interesting phenomenon related to the evolution of the couplings. Consider choosing renormalized couplings which satisfy

$$\lambda_\varphi \gg \lambda_\chi \gtrsim \lambda_{\varphi\chi} . \quad (68)$$

From (65)–(67) it is clear that according to the one-loop β -functions the couplings will flow in such a way that eventually $\lambda_{\varphi\chi}(t) > 3\lambda_\chi(t)$. For suitable initial values this occurs when all couplings are still small, so that the loop expansion ought to be valid. This means that the symmetry of the theory should be given by Eq. (40), and we see that the running of the couplings can alter the symmetry of the theory at high temperature. This effect can be exploited for model building, in that it provides a “natural” way of having phase transitions at very high temperature. For example, one can have symmetry restoration set in above the GUT scale without having to fine tune the couplings to one part in 10^{16} . Similarly, one can construct models that are broken at low temperature, get restored at some $T_c \sim \mathcal{O}(m/\sqrt{\lambda})$, and then get rebroken at a much higher temperature. For a practical application of this kind of effect to the strong CP problem and the baryon asymmetry see [4].

The above discussion was based on the assumption that the couplings evolve at high temperature according to their one-loop β -functions. We have already stated that this is approximately true, and we therefore expect that the evolution may indeed reverse the inequality $3\lambda_\chi > \lambda_{\varphi\chi}$ at high temperature. We wish to investigate the question if this really leads to symmetry breaking, as predicted by (40). Unfortunately the errors inherent in the numerical solution of our evolution equations do not allow us to vary the temperature over the 15 or so orders of magnitude necessary to achieve a significant change in the couplings. We therefore focus on the situation where one starts with $\lambda_{\varphi\chi}$ less than, but very close to, $3\lambda_\chi$, so that even a moderate change in T can alter their relationship.

Bearing in mind the above restrictions we choose $\lambda_\varphi^r = 0.1$, $\lambda_\chi^r = 1 \times 10^{-3}$, and $\lambda_{\varphi\chi}^r = 2.99 \times 10^{-3}$. If one numerically integrates equations (65)–(67) using these couplings as initial conditions at $t = 0$, the one-loop calculation (40) predicts a symmetry breaking phase transition at $T \approx 450$. The results of the Wilson RG integration are presented in Fig. 13. It is clear from

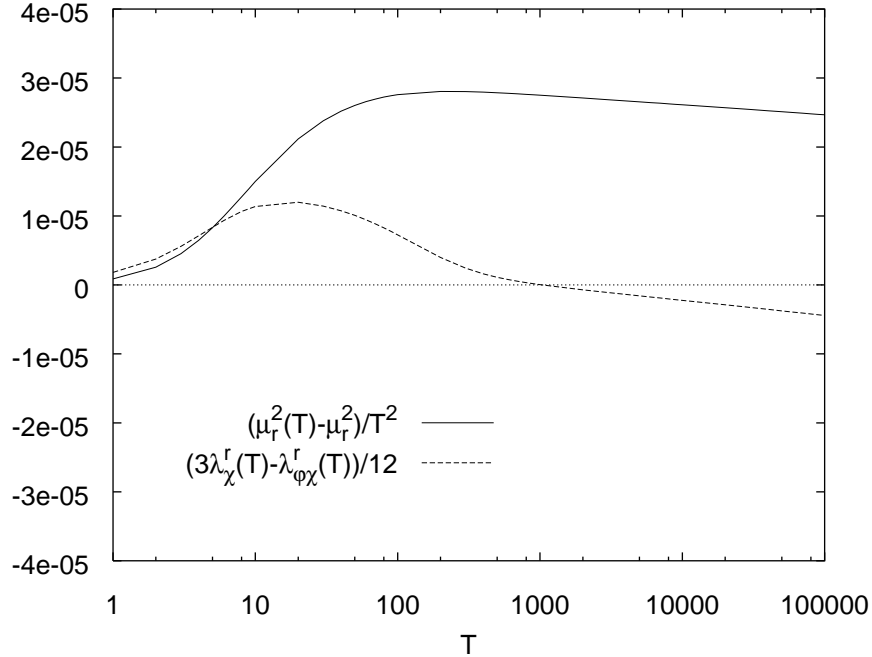


Figure 13: The temperature dependence of two combinations of parameters in the Wilson RG approach. $\mu_r^2(T)$ is rapidly increasing long after the couplings satisfy the naive inequality which predicts symmetry breaking. ($m_r^2 = \mu_r^2 = 1$, $\lambda_\varphi^r = 0.1$, $\lambda_\chi^r = 1 \times 10^{-3}$, $\lambda_{\varphi\chi}^r = 2.99 \times 10^{-3}$)

the figure that the coefficient of the T^2 term in $\mu_r^2(T)$ is not proportional to $3\lambda_\chi^r - \lambda_{\varphi\chi}^r$ as predicted by Eq. (40). In addition we see that even long after the perturbative coefficient has turned negative, $\mu_r^2(T)$ is still a rapidly increasing function of temperature. The phase transition predicted by the one-loop result is absent. This is not to say, of course, that a phase transition may not take place at much higher temperature. After all $\mu_r^2(T)/T^2$ is decreasing, and if this continues the symmetry will indeed be broken at very large T . As stated above, numerical errors prevent us from investigating this region directly.

Finally, we point out that for the initial conditions of Fig. 13, $\lambda_\chi^r(T)$ does *not* run according to its one-loop β -function over the temperature range considered. In fact, $\lambda_\chi^r(T)$ is decreasing very slowly even at $T = 10^5$. This shows that while generically the high temperature behavior of the couplings is given

by their one-loop β -functions (Fig. 12), this need not be so. The “anomalous” behavior of $\lambda_\chi^r(T)$ for the case at hand is due to the presence of two vastly different mass scales at high temperature. When $m_r^2(T)$ and $\mu_r^2(T)$ differ by several orders of magnitude, some terms in the flow equations “decouple” much earlier than others. Under these circumstances our approach is not expected to reproduce the one-loop result as the latter is blind to the presence of mass scales.

6 Conclusions

In this work we investigated the high temperature phase structure of a simple two scalar theory by solving approximately a non-perturbative RG equation for the effective potential. The solution consisted of assuming a polynomial expression for the potential and then numerically integrating the resulting coupled flow equations for the coefficients. Our main result was obtained in section 4: according to our non-perturbative method high temperature symmetry breaking (or non-restoration) does exist. In addition, we found that the phenomenon takes place roughly for those values of the couplings that satisfy the inequalities obtained from perturbation theory. The total volume of parameter space that yields high temperature symmetry breaking is only slightly reduced compared to the one-loop prediction.

We also saw that the critical temperature obtained from perturbation theory does not agree particularly well with our numerical results, even for reasonably small couplings (< 0.1). The reason for this is that the negative cross-coupling between the fields which drives the symmetry breaking must be somewhat larger than the value predicted by the loop expansion. This leads to a situation where the perturbative estimate for the critical temperature becomes totally unreliable as the cross coupling gets close to the boundary region. If one stays far away from the boundary the perturbative and numerical results approach each other to within 15%, which is about what one would expect. We also demonstrated that the critical temperature depends significantly on the value of the quartic coupling of the unbroken field, in contrast to what is predicted by the one-loop calculation.

In section 5 we discussed the behavior of the coupling constants at high temperature. In the φ^4 case the quartic coupling was shown to increase at very high temperature, but not before being significantly reduced during

an intermediate regime. For very large T the evolution was shown to be approximately given by the one-loop β -function of ordinary perturbation theory.

For the $\mathbb{Z}_2 \times \mathbb{Z}_2$ theory we focused on the effect of the running couplings on the symmetry of the theory. It was shown that generically the couplings evolve according to their one-loop β -functions at high temperature. However, we also demonstrated that it is *not* correct to draw conclusions about the symmetry of the theory based on the perturbative formula for the thermal mass and the running of the couplings. Naively this idea can be used to produce “natural” very high temperature phase transitions induced by the evolution of the couplings. Our RG approach shows that this fails for at least three reasons. First of all, even for generic initial conditions, the couplings evolve according to their one-loop β -functions only at very high T , and they are significantly renormalized by the time they reach this region. Because the couplings evolve very slowly after the initial decrease it is important to have these “initial values” in order to start the high temperature running. Using the zero temperature parameters would not suffice to get an order of magnitude estimate of T_c even if the rest of the reasoning was correct. Second, any attempt to cause high temperature symmetry breaking induced by the running of the couplings requires that one of the quartic couplings be significantly larger than the others. This introduces two widely different mass scales (the two thermal masses), with the result that some of the couplings don’t evolve according to their one-loop β -functions even at very large T . Lastly, and most importantly, we showed that even when the couplings have evolved to fulfill the naive inequality that predicts symmetry breaking, it does not happen.

The above remarks are best illustrated by the example discussed in section 5. For the renormalized parameters chosen there the one-loop evolution of the couplings (Eqs. (65)–(67)) combined with the perturbative formula for the thermal mass (Eq. (40)) predicts a symmetry breaking phase transition at $T \approx 450$. In contrast, Fig. 13 shows that the relevant thermal mass is a rapidly increasing function of temperature even at $T = 10^5$. It is possible that the symmetry will be broken at much higher T , but if this happens it will be at a temperature many orders of magnitude larger than that predicted by perturbation theory.

Finally we would like to comment on the generality of our conclusions. All of our numerical results were obtained for the simple $\mathbb{Z}_2 \times \mathbb{Z}_2$ model. However,

the differences between our RG approach and the standard one-loop treatment arise because our method correctly takes into account the decoupling of massive particles from the theory as the infrared cutoff is lowered. This feature is intrinsic to the method and independent of the particular model studied, which leads us to expect similar deviations from the perturbative results for other models.

Acknowledgements

I would like to thank Mark Alford and Brian Greene for many helpful discussions. This work was supported in part by the National Science Foundation.

Appendix: Critical Behavior

The main emphasis of this work does not rely on the details of the phase *transitions* we have studied. Rather, we have been interested in establishing the *existence* of symmetry breaking phase transitions, and in showing that the broken symmetry state can persist at arbitrarily high temperature. In this context it is only of tangential interest as to what critical exponents characterize the transition or even whether it is first or second order. In fact, we could have studied the persistence of the broken state by starting in an asymmetric vacuum at $T = 0$, in which case there would have been no phase transition at all¹². Similarly, the evolution of parameters at very high temperature does not depend on the detailed dynamics of a phase transition that has taken place at much lower T . The nature of the phase transition is important, however, in understanding the behavior of the renormalized parameters near T_c , shown in Figs. 5–7. For this reason we include here a brief discussion of the phase transitions studied in sections 3 and 4. Detailed applications of Wilson type RG equations to critical phenomena can be found in [13, 11, 14, 15, 16, 17].

We begin with the well known case of $\lambda\varphi^4$ theory. In order to study the character of a transition it is helpful to cast the flow equations into scale invariant form by using the proper dimensionless couplings. To achieve this consider the theory at high temperature. Once $\Lambda < 2\pi T$ all non-zero

¹²So long as the couplings obey the correct inequalities, see the discussion above (62).

Matsubara modes have been integrated out and we are left with an effective three dimensional theory for the zero mode (see (20)). The coupling in this theory, which has dimension one, is $\lambda_4 T$. The appropriate dimensionless mass and coupling parameters of the effective theory are hence

$$\kappa(\Lambda, T) = \frac{m^2(\Lambda, T)}{\Lambda^2} \quad (69)$$

and

$$h(\Lambda, T) = \frac{\lambda_4(\Lambda, T)T}{\Lambda}. \quad (70)$$

Rewriting equations (27) and (28) in terms of κ and h and using $t = \ln(\Lambda_0/\Lambda)$ we obtain the desired form:

$$\frac{d\kappa}{dt} = 2\kappa + \frac{3h}{2\pi^2(1+\kappa)}, \quad (71)$$

$$\frac{dh}{dt} = h - \frac{9h^2}{2\pi^2(1+\kappa)^2} \quad (72)$$

(here we have truncated by setting $\lambda_n=0$ for $n \geq 6$, as before). Equations (71) and (72) have two fixed points: the Gaussian (trivial) fixed point at $\kappa_\star = h_\star = 0$, and the Wilson fixed point (WFP) at $\kappa_\star = -1/7$ and $h_\star = 8\pi^2/49$. Linearizing around the fixed points one finds that the former is completely unstable in the IR ($t \rightarrow \infty$), while the latter is a saddle point. Hence in order for a flow to end up at the WFP one needs to fine-tune one linear combination of UV couplings, which in our case amounts to choosing $T = T_c$. Consequently $\kappa \rightarrow \kappa_\star$ and $h \rightarrow h_\star$ as $t \rightarrow \infty$ at the critical temperature, which means that the transition is second order and that

$$m_r^2(T_c) = \lim_{\Lambda \rightarrow 0} m^2(\Lambda, T_c) \sim \lim_{\Lambda \rightarrow 0} \Lambda^2 \kappa_\star = 0, \quad (73)$$

$$\lambda_{4r}(T_c) = \lim_{\Lambda \rightarrow 0} \lambda_4(\Lambda, T_c) \sim \lim_{\Lambda \rightarrow 0} \frac{\Lambda h_\star}{T_c} = 0. \quad (74)$$

This explains the behavior observed in Figs. 3–5 near T_c .

We point out that the above conclusions are independent of the parameterization used for the the flow equations, as they should be. For example, consider starting with the flow equations in the broken phase, (34) and (35). The appropriate dimensionless parameters of the effective three dimensional

theory are now $\tilde{\kappa} = \rho_0(\Lambda, T)/\Lambda T$ (recall that the field has dimension one-half in three dimensions) and $\tilde{h} = \lambda_4(\Lambda, T)T/\Lambda$. In terms of these variables (34) and (35) take a scale invariant form similar to (71) and (72). One again finds two fixed points, the Gaussian at $\tilde{\kappa}_* = 3/4\pi^2$, $\tilde{h}_* = 0$ and the WFP at $\tilde{\kappa}_* = 1/4\pi^2$, $\tilde{h}_* = 2\pi^2$. The former is again completely unstable and the latter is again a saddle point, so our above conclusions remain valid.

We now turn to the two scalar theory of section 4. Just as above we consider the effective three dimensional high temperature theory and rewrite the flow equations (57)–(61) in terms of the dimensionless variables $\kappa_\varphi = m^2(\Lambda, T)/\Lambda^2$, $\kappa_\chi = \mu^2(\Lambda, T)/\Lambda^2$, $h_\varphi = \lambda_\varphi(\Lambda, T)T/\Lambda$, $h_\chi = \lambda_\chi(\Lambda, T)T/\Lambda$, and $h_{\varphi\chi} = \lambda_{\varphi\chi}(\Lambda, T)T/\Lambda$. This results in the following set of scale invariant equations:

$$\frac{d\kappa_\varphi}{dt} = 2\kappa_\varphi + \frac{1}{2\pi^2} \left[\frac{3h_\varphi}{1+\kappa_\varphi} - \frac{h_{\varphi\chi}}{1+\kappa_\chi} \right], \quad (75)$$

$$\frac{d\kappa_\chi}{dt} = 2\kappa_\chi + \frac{1}{2\pi^2} \left[\frac{3h_\chi}{1+\kappa_\chi} - \frac{h_{\varphi\chi}}{1+\kappa_\varphi} \right], \quad (76)$$

$$\frac{dh_\varphi}{dt} = h_\varphi - \frac{1}{2\pi^2} \left[\frac{9h_\varphi^2}{(1+\kappa_\varphi)^2} + \frac{h_{\varphi\chi}^2}{(1+\kappa_\chi)^2} \right], \quad (77)$$

$$\frac{dh_\chi}{dt} = h_\chi - \frac{1}{2\pi^2} \left[\frac{9h_\chi^2}{(1+\kappa_\chi)^2} + \frac{h_{\varphi\chi}^2}{(1+\kappa_\varphi)^2} \right], \quad (78)$$

$$\frac{dh_{\varphi\chi}}{dt} = h_{\varphi\chi} - \frac{1}{2\pi^2} \left[\frac{3h_\varphi h_{\varphi\chi}}{(1+\kappa_\varphi)^2} + \frac{3h_\chi h_{\varphi\chi}}{(1+\kappa_\chi)^2} - \frac{4h_{\varphi\chi}^2}{(1+\kappa_\varphi)(1+\kappa_\chi)} \right]. \quad (79)$$

At this point one could easily determine the fixed points of the above system, investigate their stability, etc., but this is outside the scope of the present article. Rather, we note that since the χ -field remains massive during the transitions studied in section 4 it decouples in the IR, in the sense that $\kappa_\chi \rightarrow \infty$ like $1/\Lambda^2$ as $\Lambda \rightarrow 0$. For small Λ we are therefore left with the reduced system

$$\frac{d\kappa_\varphi}{dt} = 2\kappa_\varphi + \frac{1}{2\pi^2} \frac{3h_\varphi}{1+\kappa_\varphi}, \quad (80)$$

$$\frac{dh_\varphi}{dt} = h_\varphi - \frac{1}{2\pi^2} \frac{9h_\varphi^2}{(1+\kappa_\varphi)^2}, \quad (81)$$

$$\frac{dh_\chi}{dt} = h_\chi - \frac{1}{2\pi^2} \frac{h_{\varphi\chi}^2}{(1 + \kappa_\varphi)^2}, \quad (82)$$

$$\frac{dh_{\varphi\chi}}{dt} = h_{\varphi\chi} - \frac{1}{2\pi^2} \frac{3h_\varphi h_{\varphi\chi}}{(1 + \kappa_\varphi)^2}. \quad (83)$$

This system has the same two fixed points we found in the $\lambda\varphi^4$ case above, namely the trivial one and the WFP at $\kappa_\varphi = -1/7$, $h_\varphi = 8\pi^2/49$, $h_\chi = h_{\varphi\chi} = 0$. What has changed is the stability of these points. While the Gaussian fixed point is still completely unstable, the WFP now has three unstable directions instead of just one. Thus it seems that fine-tuning *one* linear combination of UV couplings (by adjusting T) is not sufficient for a flow to end up at the WFP. This, combined with the absence of other sufficiently stable fixed points, seems to indicate that the system does not undergo second order phase transitions.

Given the above analysis one may well ask why the order parameter and the couplings seem to vanish continuously near the critical temperature, as shown in Figs. 6 and 7. The reason is that κ_φ and h_φ flow to the WFP despite the instability in the other two directions in coupling space. This happens because the φ -sector of the theory completely decouples from the χ -sector (but not vice versa), as can be seen from (80)–(83). In fact, (80) and (81) are exactly the same as the equations for the simple φ^4 case, (71) and (72). Consequently all the reasoning for that case goes through and it suffices to tune one parameter (the temperature) in order to flow to the fixed point¹³. For our quartic truncation the transition is thus predicted to be second order and $m_r^2(T_c)$ and $\lambda_\varphi^r(T_c)$ flow as in (73) and (74) as $\Lambda \rightarrow 0$. The behavior of $h_{\varphi\chi}$ and h_χ at the phase transition can be found by plugging the fixed point values $\kappa_\varphi = -1/7$ and $h_\varphi = 8\pi^2/49$ into (82) and (83). These equations are then easily integrated, with the result $h_{\varphi\chi} \sim \exp(2t/3)$ and $h_\chi \sim c_1 \exp(t) - c_2 \exp(4t/3)$, where c_1 and c_2 are positive constants. For $\Lambda \rightarrow 0$ we thus obtain $\lambda_{\varphi\chi}(\Lambda, T_c) \sim \Lambda^{1/3}$ and $\lambda_\chi(\Lambda, T_c) \sim c_1 - c_2/\Lambda^{1/3}$. This

¹³It is actually not quite that simple. The fact that the WFP is a saddle point in the φ subspace indicates that one needs to fine-tune only one linear combination of couplings to flow to it. The important question is then for what values of the parameters adjusting the temperature enables one to achieve a correct linear combination. This is the question we have studied in detail in section 4, with the conclusion that the allowed parameter values are roughly those predicted by perturbation theory. In this appendix we argue only that *if* it is possible to produce a symmetry breaking phase transition by varying T , then this transition is second order and the critical behavior is equivalent to that of the \mathbb{Z}_2 model.

behavior is observed in Fig. 7. The fact that λ_χ does not go negative in the figure is simply due to the temperature resolution used. For T very close to T_c ¹⁴ one indeed finds $\lambda_\chi^r(T) < 0$.

We conclude with a few comments. First, we have verified numerically that close to T_c the RG trajectories of the full theory do get attracted to the WFP in the φ subspace. This shows that the WFP is the relevant one for our phase transitions. Second, we point out that the decoupling of the φ -sector from the χ -sector at the phase transition will occur even if the evolution equations are not truncated at quartic order in the fields as was done above. The reason for this is simple: any diagram that contributes to the running of some coupling $\lambda_\varphi^{(n)}$ (corresponding to an operator φ^n) is either built from vertices that have no χ legs or else necessarily contains closed χ -loops. The former are the same vertices present in φ^4 theory, and the latter will be highly suppressed in the IR when $\kappa_\chi = \mu^2/\Lambda^2 \rightarrow \infty$. The critical behavior of our two scalar theory near the inverse phase transitions under consideration is thus equivalent to that of the \mathbb{Z}_2 model for any polynomial truncation of the effective potential. Finally, a comment regarding the behavior of λ_χ at T_c . While it may seem odd that this coupling goes to minus infinity as the cutoff is lowered, this does not mean that the theory is unbounded. It must be remembered that without our truncation higher order terms would be present and that the four dimensional couplings do not have a simple physical interpretation in the critical theory. To illustrate this point consider the \mathbb{Z}_2 model, and the coupling λ_8 corresponding to the operator φ^8 . At high temperature the dimensionless effective three dimensional coupling relevant for the investigation of fixed points is $h_8 = T^3 \Lambda \lambda_8$. The fixed point value of h_8 turns out to be negative [14], which means that $\lambda_8(\Lambda, T_c) \rightarrow -\infty$ as $\Lambda \rightarrow 0$. In fact it is clear that all λ_n with $n \geq 8$ will diverge at T_c . The point is that the physics near the phase transition is parameterized by the critical exponents of the effective three dimensional theory and not by the four dimensional couplings.

References

- [1] D. Kirzhnits and A. Linde, Phys. Lett. B **42**, 471 (1972).

¹⁴For the parameters used in the figure this requires $|T - T_c|/T_c \sim 10^{-7}$.

- [2] S. Weinberg, Phys. Rev. D **9**, 3357 (1974).
- [3] L. Dolan and R. Jackiw, Phys. Rev. D **9**, 3320 (1974).
- [4] R. N. Mohapatra and G. Senjanovic, Phys. Lett. B **89**, 57 (1979).
- [5] P. Salomonson, B.-S. Skagerstam, and A. Stern, Phys. Lett. B **151**, 243 (1985); P. Langacker and S. Y. Pi, Phys. Rev. Lett. **45**, 1 (1980).
- [6] G. Dvali, A. Melfo, and G. Senjanovic, Report No. IC-95-145, hep-ph/9507230, 1995 (unpublished); G. Bimonte and G. Lozano, Report No. IC-95-220, hep-th/9509060, 1995 (unpublished).
- [7] S. Dodelson and L. M. Widrow, Mod. Phys. Lett. A **5** 1623 (1990); Phys. Rev. D **42**, 326 (1990), Phys. Rev. Lett. **64**, 340 (1990); S. Dodelson, B. R. Greene, and L. M. Widrow, Nucl. Phys. B **372** 467 (1992).
- [8] J. Lee and I. Koh, hep-ph/9506415, 1995 (unpublished).
- [9] Y. Fujimoto and S. Sakakibara, Phys. Lett. B **151**, 260 (1985); E. Manesis and S. Sakakibara, *ibid.* **157**, 287 (1985); K. G. Klimenko, Theor. Math. Phys. **80**, 929 (1989); Z. Phys. C **43**, 581 (1989); M. P. Grabowski, *ibid.* **48**, 505 (1990).
- [10] T. R. Morris, Int. J. Mod. Phys. A **9**, 2411 (1994). Also contains a brief history of exact RG equations and many references to the original papers.
- [11] T. R. Morris, Phys. Lett. B **334**, 355 (1994).
- [12] C. Wetterich, Phys. Lett. B **301**, 90 (1993); M. Bonini, M. D’Attanasio, G. Marchesini, Nucl. Phys. B **409**, 441 (1993).
- [13] M. Grater and C. Wetterich, Phys. Rev. Lett. **75**, 378 (1995); M. Alford, Nucl. Phys. B **417**, 527 (1994).
- [14] M. Alford, Phys. Lett. B **336**, 237 (1994).
- [15] N. Tetradis and C. Wetterich, Nucl. Phys. B **398**, 659 (1993).
- [16] S. Bornholdt, N. Tetradis, and C. Wetterich, Report No. OUTP-95-02-P, hep-ph/9503282, 1995 (unpublished).

- [17] N. Tetradis and C. Wetterich, Nucl. Phys. B **422**, 541 (1994).
- [18] T. R. Morris, Report No. SHEP-95-21, hep-th/9508017, 1995 (unpublished).
- [19] S.-B. Liao and J. Polonyi, Phys. Rev. D **51**, 748 (1995).
- [20] S.-B. Liao and M. Strickland, Phys. Rev. D **52**, 3653 (1995).
- [21] T. R. Morris, Phys. Lett. B **329**, 241 (1994).
- [22] J. Polchinski, Nucl. Phys. B **231**, 269 (1984).
- [23] T. W. Kephart, T. J. Weiler and T.-C. Yuan, Nucl. Phys. **B330**, 705 (1990).
- [24] K. B. Josesh, V. C. Kuriakose, and M. Sabir, Phys. Lett. B **115**, 120 (1982); Y. Fujimoto, K. Ideura, Y. Nakano, and H. Yoneyama, *ibid.* **167**, 406 (1986); P. Elmfors, Z. Phys. C **56**, 601 (1992); F. Freire and C. R. Stephens, *ibid.* **60**, 127 (1993); reference [20].
- [25] See, e.g., S.-P. Chia, Int. J. Mod. Phys. A **2**, 713 (1987); O. J. P. Eboli and G. C. Marques, Phys. Lett. B **162**, 189 (1985).
- [26] See, e.g., H. A. Weldon, Phys. Lett. B **174**, 427 (1986); reference [27].
- [27] P. Fendley, Phys. Lett. B **196**, 175 (1987).
- [28] See, e.g., S. Mohan, Phys. Lett. B **307**, 367 (1993); P. Salomonson and B.-S. K. Skagerstam, *ibid.* **155**, 100 (1985); reference [4].